

# A novel approach for quantifying similarities between different debris flow sites using field investigations and numerical modelling

Minu Treesa Abraham<sup>1,2</sup>  | Neelima Satyam<sup>1</sup> | Biswajeet Pradhan<sup>3,4</sup>

<sup>1</sup>Department of Civil Engineering, Indian Institute of Technology Indore, Indore, India

<sup>2</sup>Methods for Model-based Development in Computational Engineering, RWTH Aachen University, Aachen, Germany

<sup>3</sup>Centre for Advanced Modelling and Geospatial Information Systems (CAMGIS), School of Civil and Environmental Engineering, University of Technology Sydney, Sydney, New South Wales, Australia

<sup>4</sup>Earth Observation Centre, Institute of Climate Change, Universiti Kebangsaan Malaysia, Bangi, Malaysia

## Correspondence

Biswajeet Pradhan, Centre for Advanced Modelling and Geospatial Information Systems (CAMGIS), School of Civil and Environmental Engineering, University of Technology Sydney, Sydney, NSW 2007, Australia.

Email: [biswajeet.pradhan@uts.edu.au](mailto:biswajeet.pradhan@uts.edu.au)

## Funding information

Indian Institute of Technology Indore; University of Technology Sydney

## Abstract

Debris flows are geomorphological processes that affect the landscape evolution process of any region. In this study, an integrated methodology is proposed to identify the chance of further debris flows and quantify the similarities between debris flow locations, materials and rheology, using field and laboratory investigations and remote sensing data. The method was tested for four failure-triggered debris flow sites in the Western Ghats of India, using dimensionless parametric similarity values ranging from 0 to 1. The maximum parametric similarity was observed as 0.84 when comparing the flow accumulation values of Sites 3 and 4, and the maximum overall site similarity was 0.68. The calibrated rheological parameters of one site were found to be satisfactory in modelling the shape of debris flow at all other sites. The findings can be used to identify similar hotspots in the region and to simulate debris flows for quantitative hazard assessment.

## KEYWORDS

debris flows, landslides, rheology, similarity

## 1 | INTRODUCTION

The word “debris flow” refers to a common and critical hazard in steep terrain. Debris flows can be broadly classified into two categories: those triggered by failure and those triggered by runoff (Kean et al., 2013). In runoff-triggered debris flows, the loose debris deposits on steep channels get eroded during heavy rainfall. In failure-triggered debris flows, a slide or fall from a steep slope or spontaneous instability of the steep stream bed could trigger the event. The loose debris deposits along the path of a debris flow will

act as erodible material for another runoff-triggered debris flow. In the case of soils with higher fine fractions, the event is triggered by the combination of heavy rainfall and shallow failure at higher elevations (Baggio et al., 2021). But when the deposits are very loose, a flux in the already disturbed channel can affect the stability of the banks and bed and progress as a debris flow (Gregoretti & Fontana, 2008). Concentrated overland flow in steep basins will result in the mobilization of such deposits, leading to debris flow activity (Berti & Simoni, 2005). The temporal forecasting of such events relies upon the critical intensity-duration conditions of rainfall (Kean

This is an open access article under the terms of the [Creative Commons Attribution-NonCommercial-NoDerivs](https://creativecommons.org/licenses/by-nc-nd/4.0/) License, which permits use and distribution in any medium, provided the original work is properly cited, the use is non-commercial and no modifications or adaptations are made.

© 2023 The Authors. *Terra Nova* published by John Wiley & Sons Ltd.

et al., 2013). Further, the spatial extent and the impact of flow can be quantified using numerical modelling tools (Mergili et al., 2017; Trujillo-Vela et al., 2022). However, the applicability of such models is limited in the prediction of future events due to the limitations in calibrating the complex rheological parameters (Zhao & Kowalski, 2022). It is not well studied if the rheological parameters calibrated for one site can be used for the prediction of the shape of debris flows at other sites.

This study attempts to evaluate the similarities between these four debris flow sites in terms of material properties, topography and rheological parameters. The possible use of rheological parameters calibrated for one debris flow for the simulation of other debris flows at similar sites is evaluated. The findings can aid in predicting the impact area of debris flows at 'similar sites' and thereby identifying the elements exposed to risk. Also, the critical rainfall conditions that can lead to debris flows in the region are identified to support the early warning decisions.

## 2 | DESCRIPTION OF SITES

Four different long-runout debris flow sites in the very high landslide-susceptible zones of the Wayanad district in Kerala, India (Figure 1) were selected for the study. Two sites from the southwestern part of the district (Kurichermala and Puthumala) and two from the northwestern part (Maniyankunnu and Pancharakkolli) are considered.

### Statement of significance

Debris flow modelling is considered an expert field due to the complexities associated with it. No studies have been conducted on quantifying the similarities between different debris flow sites. Identifying similar sites can help in the forward analysis of debris flows and thereby use numerical modelling for disaster risk reduction. The method is tested for four debris flow locations in Kerala, India, and the results indicate that the topographical and material properties of these locations are similar, and hence the same rheological parameters can effectively model the shape of debris flows in the region. The study provides new insights on debris flow modelling, which are useful in debris flow hazard assessment and identification of elements exposed to risk.

At Kurichermala (Site 1), the debris flow initiated from the forest area in August 2018, devastating more than 150 acres of land. The region recorded extremely heavy rainfall on these days, as the nearest rain gauge recorded a total of 330mm of rainfall on 8th and 9th August 2018. There are four channels separated immediately after an intermediate zone of deposition, where massive rock pieces and

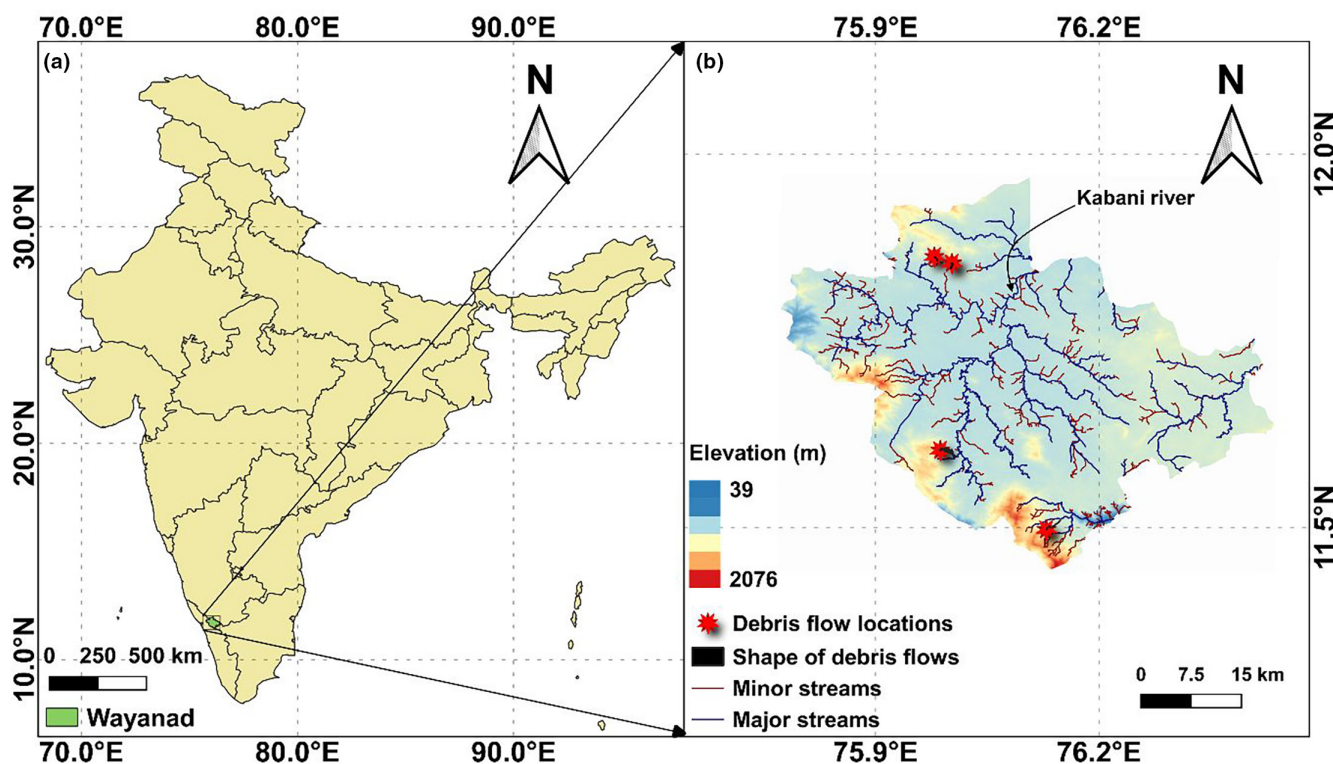


FIGURE 1 Location details. (a) India and (b) Wayanad.

thick, soft soil deposits were observed. The longest channel travelled a distance of 3.1 km from the crown.

At Puthumala (Site 2), multiple landslides occurred on 8th August 2019. Many shallow landslides, minor debris flows and rock falls have occurred in the vicinity of the major debris flow location. The crown of the primary channel is covered with weathered rock and laterite soil. The crown has two flanks: one translational rockslide and a rotational debris slide.

At Maniyankunnu (Site 3), minor slope failures occurred on 9th August 2018. The debris flow occurred on 17th August 2018. Deposition occurred along the sides of the flow path immediately after the crown, creating the channel for a first-order stream along the runout path.

Site 3 and Pancharakkolli (Site 4) are located nearby, and the major debris flow at Site 4 occurred on 16th August 2018. The flow is oriented from northwest to southeast, with a total runout distance of 820 m. The initial deposition zone is immediately below the crown, and another intermediate zone of deposition is observed parallel to the rotational debris slide.

### 3 | METHODOLOGY

An integrated methodology including statistical, geophysical and geotechnical aspects is explored (Figure 2). The first step in the process is the collection of a historical database of landslides and their major triggering factor, rainfall. The major debris flow events

were identified from the database, and the intensity( $I$ )-duration( $D_h$ ) threshold equation was derived for the initiation of debris flows in the region using a frequentist approach. For deriving the rainfall thresholds, a debris flow event is defined as one or more debris flows that occurred on the same day within the reference area covering the nearest rain gauge. The rainfall data were collected from four different rain gauges in the region from 2010 to 2018, and the responsible rainfall event was identified using a proximity-based approach, using Thiessen polygons (Abraham et al., 2020). From the prepared database and satellite images, the locations for a detailed study were selected.

In the second stage, detailed field investigations were conducted at the four sites to understand the subsurface profile and soil characteristics. Vertical electrical surveys (VESs) were performed at multiple locations at each site (Figure 3) to understand the thickness of soft soil above bedrock and to evaluate the chances of future debris flows. A standard penetration test (SPT) was conducted at the lowest elevation VES point to collect soil and rock samples from the site and to assess the reliability of the VES. Soil samples were collected from different depths at SPT locations and also from ground level, from VES locations and from the longitudinal section connecting all VES points (Figure 3), such that there are 50 sampling points at each location.

The third stage involves studies using remote sensing data. The digital elevation maps (DEMs) were used for the numerical modelling of debris flows and to derive the slope, elevation, aspect and flow accumulation values for each site. The results were then used

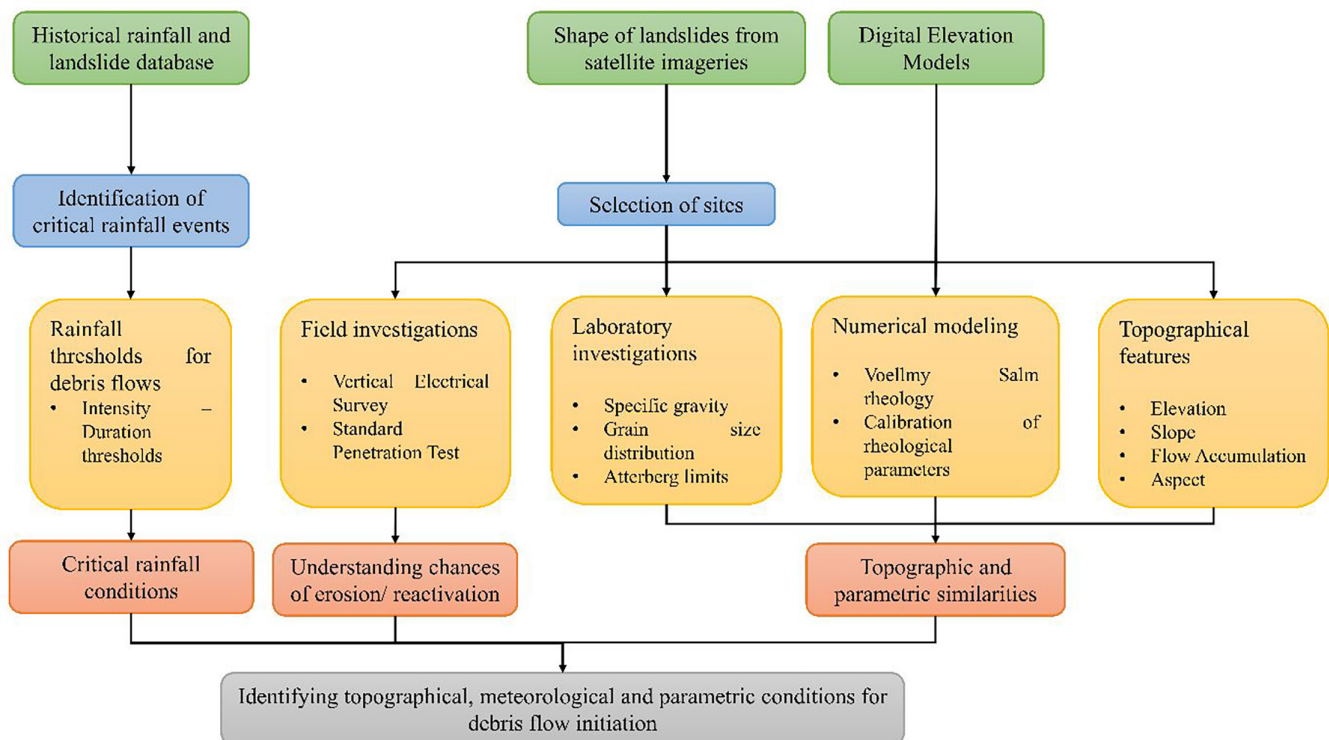


FIGURE 2 Schematic diagram showing the methodology of the study.

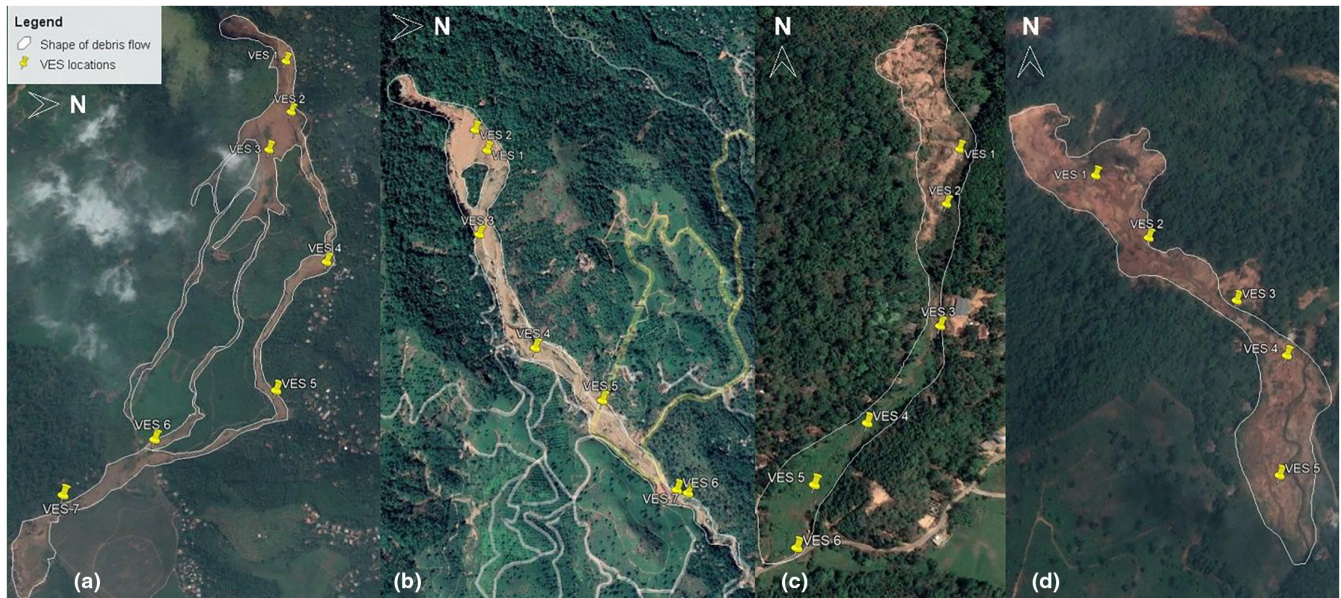


FIGURE 3 The shape of debris flows with the locations of VES. (a) Site 1, (b) Site 2, (c) Site 3 and (d) Site 4.

to quantify the similarity of sites through confidence ellipses. The similarity was determined using the term parameter similarity degree (Han et al., 2022) ( $S_{para}$ ), using the following equation:

$$S_{para} = \frac{A_{oa}}{A_{e1} + A_{e2} - A_{oa}} \quad (1)$$

where  $A_{oa}$  is the area of intersection of the two ellipses and  $A_{e1}$  and  $A_{e2}$  are the total areas of the two ellipses considered. From the  $S_{para}$  values of individual parameters, the overall site similarity can be calculated as the mean of all  $S_{para}$  values.

In the fourth stage, back-analysis of debris flows was conducted using RAMMS (Christen et al., 2010) to calibrate the rheological parameters and understand the similarity of the same across different sites. The model uses single-phase flow with Voellmy-Salm rheology, and the rheological parameters to be calibrated are the turbulent friction ( $\xi$ ) and the dry-Coulomb friction ( $\mu$ ). The modelling was carried out using 12.5 m DEM from Alos Palsar, and the calibration was carried out using the procedure explained in Abraham et al., 2021, using the structural similarity of the observed and simulated shapes of debris flows. Further, all similarities were evaluated in detail to understand if the sites were similar or not. Finally, the rainfall thresholds along with calibrated rheological parameters provide the spatio-temporal patterns of future debris flow events possible in the study area.

## 4 | RESULTS AND DISCUSSION

As the major triggering factor, identifying the critical rainfall conditions that may trigger debris flows in the region is crucial from a disaster management perspective. Based on the distribution of data, the threshold line with a 5% exceedance probability was calculated

as  $I = 6.43D_h^{-0.33}$ , where  $I$  is in mm/h and  $D_h$  is in hours, using 14 debris flow events identified during the studied duration. The database should be continuously updated with more events to use the threshold for early warning. Once this threshold is expected to exceed based on rainfall forecasts, utmost care should be taken to issue a warning for the possible occurrence of debris flows in the region.

The results of VES and SPT divide the subsurface into three distinct layers (Figure 4). A topsoil layer of loose debris with boulders and fragmented rocks ( $D$ ), a layer of thick sand-silt-clay matrix ( $S$ ) and the bedrock beneath the overburden.

The thickness of  $D$  is maximum at Site 1 (Figure 5), 9.62 m, at an intermediate deposition zone, at an elevation of around 935 m. The thickness of  $D$  is maximum at the higher elevation parts and lesser at the zones of deposition in all sites due to the presence of fine fraction, which gets densified faster. More than 600,000 m<sup>3</sup> of loose debris material is available at both Sites 1 and 2, which may get eroded slowly. At Sites 3 and 4, the quantity of  $D$  is much lesser (approximately 65,000 m<sup>3</sup> and 85,000 m<sup>3</sup>, respectively). From the grain size analysis of soil samples, it was found that the percentage of fines in the soil sample increases along with the increase in distance from the crown and vertically downwards from the surface. The coarse-grained particles remain loose and are prone to higher erosion rates, while the fine grain composition increases in deeper layers of soil. Layer  $S$  is composed more of finer particles and is rich in mineral content, which allows fast regrowth of vegetation. Chances for retrogressive failure are higher at Sites 1 and 4 (Figure 5a). The soil particles from all other sites except Site 2 are primarily composed of coarse-grained particles with a significant fine content (more than 12%). Considering the soil composition, the liquid limit (LL), plastic limit (PL), specific gravity ( $G$ ) and percentage fines ( $P_{fines}$ ) were used for quantifying the similarities between sites.

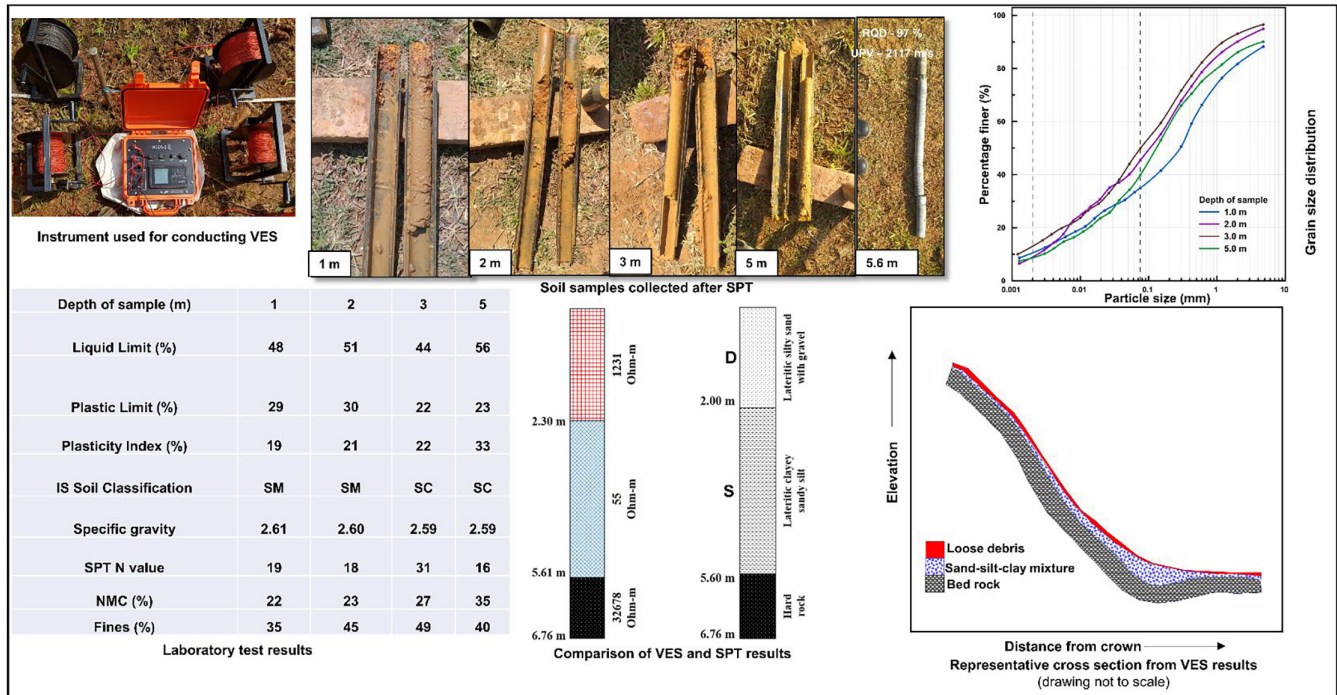


FIGURE 4 An example from Site 2 summarizing the results of geophysical and geotechnical investigations.

From the topographical data, slope (SI) and flow accumulation (FA) were found to be the critical governing factors determining the flow path, as evident from Figure 6. The slope of the terrain and its orientation control the direction of flow, from which FA values can be derived.

Employing the confidence ellipse, it was found that all the sites show an overall similarity of more than 0.5, which is quantified using  $S_{para}$  (Han et al., 2022). The structural similarity Index (SSIM) values were obtained after comparing the simulated shapes with the actual shape of debris flow. An example of plotting a confidence ellipse is shown in Figure 7a for the normalized random variables corresponding to FA ( $R_{FA}$ ) and distance from the crown ( $R_d$ ).

The similarity is maximum for FA and lowest for percentage fines, as shown in Table 1. There is a well-accepted agreement that the conditioning factors that have triggered landslides in the past can lead to landslides in the future as well. The natural flow path is regained through the debris flows, resulting in the formation of new minor-order streams.

The area affected by debris flows can be understood using numerical modelling, but the rheological parametric inputs are difficult to quantify without back-analysis. As our objective is to identify the elements exposed to risk, the shape of the debris flow is the most critical aspect. The modelling was done with block release after calculating the release area from field observations. At Sites 3 and 4, the flow has happened without significant bed entrainment. After calibrating the parameters, the values for each site were used for the back analysis of all other sites to evaluate the possible difference in predicted shape, and the results are shown in Figure 8. The optimum values of turbulent friction for Site 1, Site 2, Site 3 and Site 4 are

100m/s<sup>2</sup>, 300m/s<sup>2</sup>, 400m/s<sup>2</sup> and 300m/s<sup>2</sup>, respectively. The corresponding values of the dry-Coulomb friction are 0.01, 0.01, 0.03 and 0.03.

From Figure 8, it is evident that the calibrated friction parameters for one site can satisfactorily predict the shape of other debris flows as well, which indicates that the turbulent friction values ranging from 100m/s<sup>2</sup> to 400m/s<sup>2</sup> and dry Coulomb friction values ranging from 0.01 to 0.03 can be used to simulate the debris flows in the region. The calibrated values are satisfactory to delineate the area under threat due to debris flows, with a minimum SSIM value of 0.59. It is interesting to note that, for Site 3, all the parameters simulated very similar shapes when compared with the actual shape of debris flow, and the SSIM values were lowest for Site 1. This is accounted for by the complexities associated with the flow paths, governed by the slope, aspect and FA values. Site 3 and Site 2 have the least complex flow paths and have maximum topographical similarities with all the other sites. This has clearly been reflected in numerical modelling as well.

From the results, it can be understood that the selected site shows similarities in topography and material properties, and the calibrated rheological parameters for one study can be used for prediction of the shape of debris flows at other sites. The similarity in rheological properties can be attributed to the similarities in topography of the studied sites; however, this needs a larger database of detailed debris flow case studies to arrive at a generalized conclusion. Thus, the area affected by debris flows in the same catchment at similar sites can be predicted using the calibrated rheological parameters using a 12.5-m resolution DEM, and the occurrence of such events can be forecasted using the rainfall threshold derived in this study.

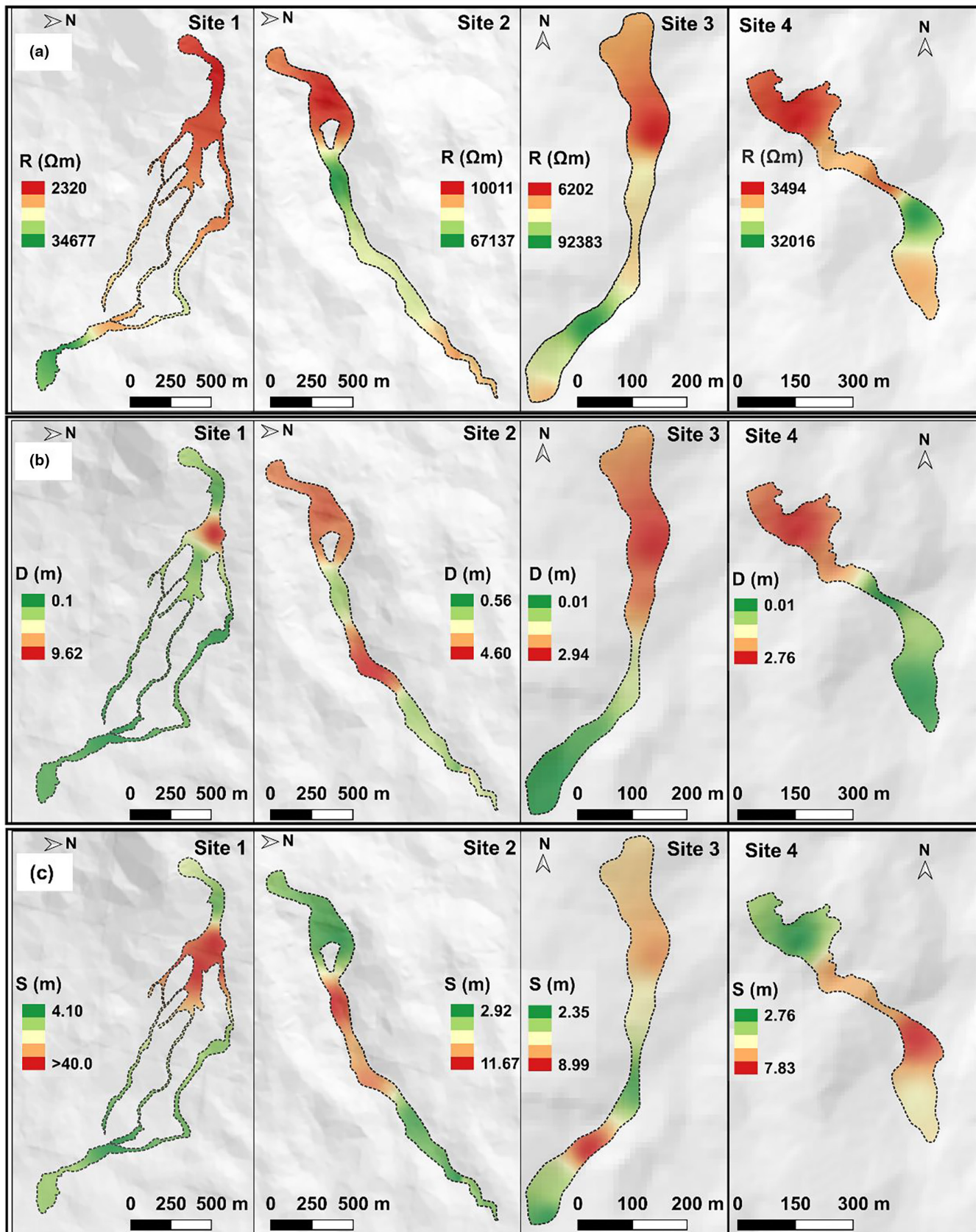


FIGURE 5 Results of VES. (a) Resistivity values of bedrock, (b) thickness of loose debris material with boulders and (c) thickness of soft soil overburden above bedrock.

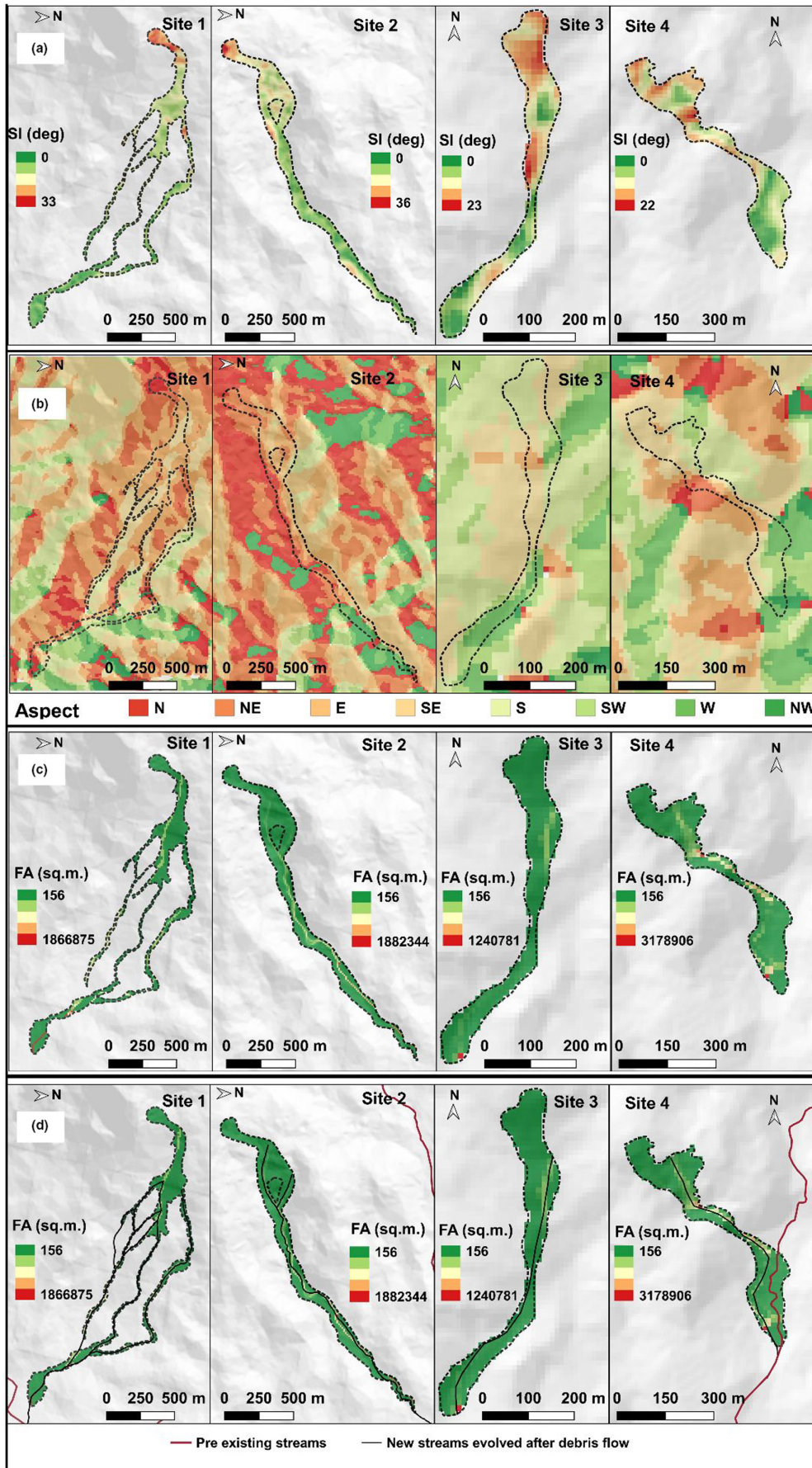


FIGURE 6 Topographical features considered for the quantification of site similarity. (a) Slope map, (b) Aspect map, (c) flow accumulation map, and (d) details of newly evolved streams after debris flows.

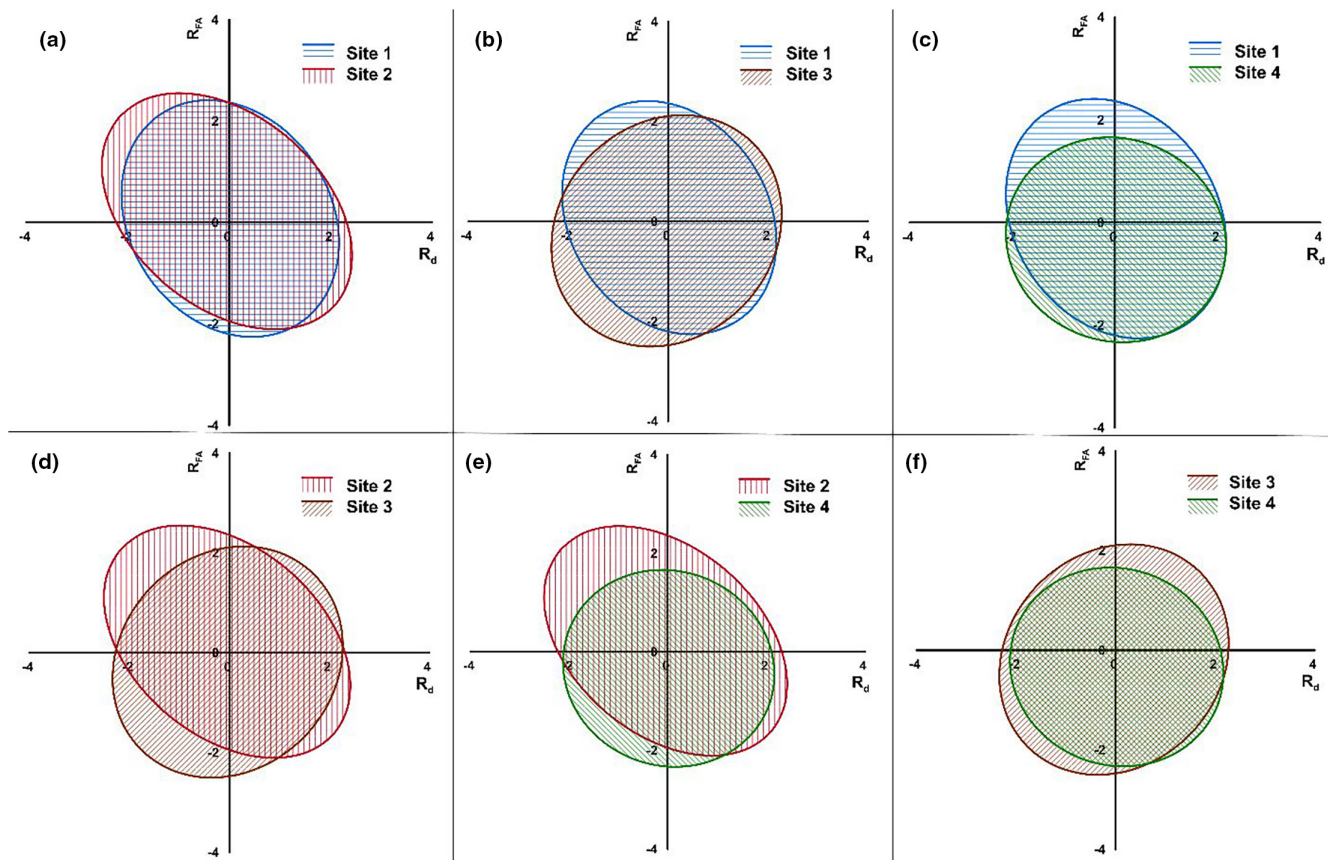


FIGURE 7 Confidence ellipses plotted for the flow accumulation values at different sites to quantify similarity. (a) Site 1–Site 2, (b) Site 1–Site 3, (c) Site 1–Site 4, (d) Site 2–Site 3, (e) Site 2–Site 4 and (f) Site 3–Site 4.

	Site 1–Site 2	Site 1–Site 3	Site 1–Site 4	Site 2–Site 3	Site 2–Site 4	Site 3–Site 4
FA	0.83	0.74	0.82	0.68	0.77	0.84
Slope	0.49	0.51	0.41	0.84	0.62	0.68
Liquid limit	0.56	0.52	0.52	0.68	0.57	0.57
Plastic limit	0.77	0.65	0.59	0.67	0.56	0.66
Specific gravity	0.53	0.54	0.65	0.67	0.59	0.61
Percentage fines	0.47	0.49	0.43	0.56	0.44	0.73
Similarity of topographical features	0.66	0.63	0.62	0.76	0.70	0.76
Similarity of soil properties	0.58	0.55	0.55	0.65	0.54	0.64
Overall site similarity	0.61	0.57	0.57	0.68	0.59	0.68

TABLE 1  $S_{para}$  values obtained for different parameters and overall site similarity.

A major limitation of the study is the non-availability of aerial surveys and the lack of understanding of topographic changes after the debris flows. The quality of the DEM and the topographic effects significantly affect the performance of the numerical model (Baselt et al., 2022). The DEM can also help in understanding the terrain characteristics post-debris flow (Dietrich & Krautblatter, 2019; Simoni et al., 2020), and the post-event evaluation

should include both aerial and sub-surface investigations. Such investigations can give better insights on the erosion, deposition and volume changes that have happened due to the flow. Also, the study can be further extended by exploring more similarities in terms of geology and by exploring different approaches for extrapolating soil thickness (Catani et al., 2010; Del Soldato et al., 2018; Saulnier et al., 1997).



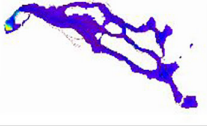

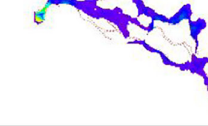
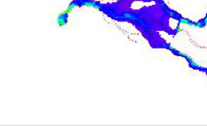
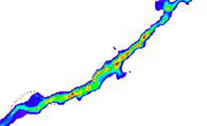
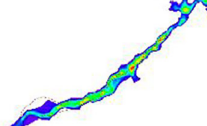
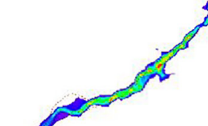
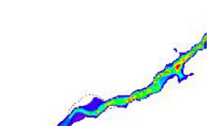




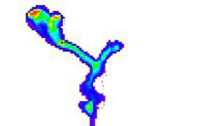
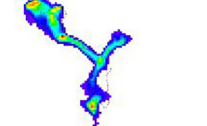
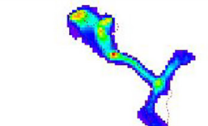
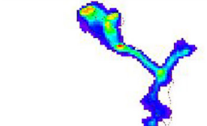
$\xi$ ( $\text{ms}^{-2}$ )	100	300	400	300
$\mu$	0.01	0.01	0.03	0.03
Site 1				
	SSIM: 0.626	SSIM: 0.610	SSIM: 0.592	SSIM: 0.586
Site 2				
	SSIM: 0.838	SSIM: 0.855	SSIM: 0.841	SSIM: 0.843
Site 3				
	SSIM: 0.685	SSIM: 0.687	SSIM: 0.695	SSIM: 0.686
Site 4				
	SSIM: 0.665	SSIM: 0.702	SSIM: 0.701	SSIM: 0.740

FIGURE 8 Shape of debris flow using numerical modelling (all oriented north vertically upwards).

## 5 | CONCLUSIONS

The study investigates the meteorological, topographical, material and rheological properties that trigger debris flows in Wayanad district, Kerala, India. Four debris flow locations were selected and investigated in detail to understand the material and subsurface properties. From the investigations, it was understood that the chances of further retrogressive failures are higher at Sites 1 and 4. All four locations were found to have the highest similarity in terms of FA values, and the overall site similarity in terms of values was the maximum between Sites 2 and 3 and Sites 3 and 4, with a similarity value of 0.68. The overall topographic similarity and material similarity between all sites were found to be greater than 0.5, and the SSIM values for simulated and observed debris flow shapes were also found to be greater than 0.5 in all the cases. This indicates that the turbulent friction values ranging from  $100\text{ m/s}^2$  to  $400\text{ m/s}^2$  and the dry Coulomb friction values ranging from 0.01 to 0.03 can satisfactorily reproduce the impact area of debris flows in the region using a 12.5-m resolution DEM. The calibrated values can be used to identify similar sites and to conduct a forward analysis of debris flows to identify the elements exposed to risk.

## ACKNOWLEDGEMENTS

The authors acknowledge the funding received from the Department of Space, Government of India, under grant number ISRO/RES/4/663/18-19. The authors are also grateful to Dr. A. Kowsigan (Commissioner, Disaster Management Kerala) and Dr. Sekhar Lukose Kuriakose (Member Secretary, Kerala State Disaster Management Authority [ex-officio]) for granting us permission to conduct the geotechnical investigations in the field. The support from the staff of Kerala State Disaster Management Authority, District Disaster Management Authority, Wayanad and District Forest Office, Wayanad was extremely helpful for the field work. The authors would also like to acknowledge the support from Dr. Anil Joseph (Managing Partner, Engineers Diagnostic Centre [P] Ltd., Kerala) and Geoservices Mairitme Pvt., Ltd. Mumbai, during the field investigations.

## CONFLICT OF INTEREST STATEMENT

The authors declare no conflicts of interest.

## DATA AVAILABILITY STATEMENT

The data that support the findings of this study are available from the corresponding author upon reasonable request.

## ORCID

Minu Treesa Abraham  <https://orcid.org/0000-0002-2540-8681>

## REFERENCES

- Abraham, M. T., Satyam, N., Reddy, S. K. P., & Pradhan, B. (2021). Runout modeling and calibration of friction parameters of Kurichermala debris flow, India. *Landslides*, 18, 737–754. <https://doi.org/10.1007/s10346-020-01540-1>
- Abraham, M. T., Satyam, N., Rosi, A., Pradhan, B., & Segoni, S. (2020). The selection of rain gauges and rainfall parameters in estimating intensity-duration thresholds for landslide occurrence: Case study from Wayanad (India). *Water*, 12, 1000. <https://doi.org/10.3390/w12041000>
- Baggio, T., Mergili, M., & D'Agostino, V. (2021). Advances in the simulation of debris flow erosion: The case study of the Rio Gere (Italy) event of the 4th august 2017. *Geomorphology*, 381, 107664. <https://doi.org/10.1016/j.geomorph.2021.107664>
- Baselt, I., de Oliveira, G. Q., Fischer, J.-T., & Pudasaini, S. P. (2022). Deposition morphology in large-scale laboratory stony debris flows. *Geomorphology*, 396, 107992. <https://doi.org/10.1016/j.geomorph.2021.107992>
- Berti, M., & Simoni, A. (2005). Experimental evidences and numerical modelling of debris flow initiated by channel runoff. *Landslides*, 2, 171–182. <https://doi.org/10.1007/s10346-005-0062-4>
- Catani, F., Segoni, S., & Falorni, G. (2010). An empirical geomorphology-based approach to the spatial prediction of soil thickness at catchment scale. *Water Resources Research*, 46(5), W05508. <https://doi.org/10.1029/2008WR007450>
- Christen, M., Kowalski, J., & Bartelt, P. (2010). RAMMS: Numerical simulation of dense snow avalanches in three-dimensional terrain. *Cold Regions Science and Technology*, 63, 1–14. <https://doi.org/10.1016/j.coldregions.2010.04.005>
- Del Soldato, M., Pazzi, V., Segoni, S., De Vita, P., Tofani, V., & Moretti, S. (2018). Spatial modeling of pyroclastic cover deposit thickness (depth to bedrock) in peri-volcanic areas of Campania (southern Italy). *Earth Surface Processes and Landforms*, 43(9), 1757–1767. <https://doi.org/10.1002/esp.4350>
- Dietrich, A., & Krautblatter, M. (2019). Deciphering controls for debris-flow erosion derived from a LiDAR-recorded extreme event and a calibrated numerical model (Roßbichelbach, Germany). *Earth Surface Processes and Landforms*, 44, 1346–1361. <https://doi.org/10.1002/esp.4578>
- Gregoretti, C., & Fontana, G. D. (2008). The triggering of debris flow due to channel-bed failure in some alpine headwater basins of the Dolomites: Analyses of critical runoff. *Hydrological Processes*, 22, 2248–2263. <https://doi.org/10.1002/hyp.6821>
- Han, L., Wang, L., Ding, X., Wen, H., Yuan, X., & Zhang, W. (2022). Similarity quantification of soil parametric data and sites using confidence ellipses. *Geoscience Frontiers*, 13, 101280. <https://doi.org/10.1016/j.gsf.2021.101280>
- Kean, J. W., McCoy, S. W., Tucker, G. E., Staley, D. M., & Coe, J. A. (2013). Runoff-generated debris flows: Observations and modeling of surge initiation, magnitude, and frequency. *Journal of Geophysical Research: Earth Surface*, 118, 2190–2207. <https://doi.org/10.1002/jgrf.20148>
- Mergili, M., Fischer, J.-T., Krenn, J., & Pudasaini, S. P. (2017). R.avaflow v1, an advanced open-source computational framework for the propagation and interaction of two-phase mass flows. *Geoscientific Model Development*, 10, 553–569. <https://doi.org/10.5194/gmd-10-553-2017>
- Saulnier, G. M., Beven, K., & Obleed, C. (1997). Including spatially variable effective soil depths in TOPMODEL. *Journal of Hydrology*, 202(1–4), 158–172. [https://doi.org/10.1016/S0022-1694\(97\)00059-0](https://doi.org/10.1016/S0022-1694(97)00059-0)
- Simoni, A., Bernard, M., Berti, M., Boreggio, M., Lanzoni, S., Stancanelli, L. M., & Gregoretti, C. (2020). Runoff-generated debris flows: Observation of initiation conditions and erosion–deposition dynamics along the channel at Cancia (eastern Italian Alps). *Earth Surface Processes and Landforms*, 45, 3556–3571. <https://doi.org/10.1002/esp.4981>
- Trujillo-Vela, M. G., Ramos-Cañón, A. M., Escobar-Vargas, J. A., & Galindo-Torres, S. A. (2022). An overview of debris-flow mathematical modelling. *Earth-Science Reviews*, 232, 104135. <https://doi.org/10.1016/j.earscirev.2022.104135>
- Zhao, H., & Kowalski, J. (2022). Bayesian active learning for parameter calibration of landslide run-out models. *Landslides*, 19, 2033–2045. <https://doi.org/10.1007/s10346-022-01857-z>

**How to cite this article:** Abraham, M. T., Satyam, N., & Pradhan, B. (2023). A novel approach for quantifying similarities between different debris flow sites using field investigations and numerical modelling. *Terra Nova*, 00, 1–10. <https://doi.org/10.1111/ter.12679>